Available online at www.sciencedirect.com
ScienceDirect
Applied Catalysis B: Environmental 79 (2007) 179–185
APPLIED CATALYSIS B: ENVIRONMENTAL
www.elsevier.com/locate/apcatb

Two-component transparent TiO_2/SiO_2 and TiO_2/PDMS films as efficient photocatalysts for environmental cleaning

Petra Novotná [a], Jiří Zita [a], Josef Krýsa [a,*], Vít Kalousek [b], Jiří Rathouský [b]

[a] *Institute of Chemical Technology Prague, Department of Inorganic Technology, Technická 5, CZ-166 28 Prague 6, Czech Republic*
[b] *J. Heyrovský Institute of Physical Chemistry of AS CR, v.v.i., Dolejškova 3, CZ-182 23 Prague 8, Czech Republic*

Received 20 June 2007; received in revised form 10 October 2007; accepted 15 October 2007
Available online 22 October 2007

Abstract

TiO_2 films modified either with polydimethylsiloxane (PDMS) or SiO_2 were prepared by a sol–gel method combined with dip-coating. TiO_2/PDMS films have a lower abrasion resistance and are more hydrophobic than the TiO_2/SiO_2 ones. As the TiO_2/PDMS films calcined at 350–450 °C exhibit developed micro-mesoporosity, they adsorb considerable amounts of methylene blue from its water solution. However, their photocatalytic activity in the decomposition of this dye is very low. On the contrary, these films are highly active in the degradation of the layers of methyl stearate. This efficiency variation is explained by the film-developed porosity. The films modified with SiO_2 have very good abrasion resistance and can be easily converted by weak UV-illumination into substantially stable superhydrophilic state. Furthermore, they exhibit good photocatalytic properties in both test reactions.

Keywords: TiO_2; SiO_2; PDMS; Thin film; Hydrophilicity; Photoactivity

1. Introduction

Sol–gel processing enables to obtain various shapes directly from the gel state, such as monoliths, films, fibers and monosized powders, and to control the composition and microstructure at low processing temperatures [1]. Thin films benefit from most of the just cited advantages while avoiding the disadvantages of the high cost of the raw materials, shrinkage that accompanies drying and sintering, and the formation of cracks. Performance characteristics of multi-component films can sometimes be derived from those of individual components, often, however, synergistic effects occur, which may substantially modify their performance.

Thin transparent layers containing TiO_2 have been intensively studied due to their interesting application potential in, e.g., photocatalytic purification of water and air [2,3]. To improve their mechanical properties, SiO_2 [4,5] or siloxanes [6,7] have been added. Additionally, doping with suitable metals, such as Sn [8], Cu [9] and Ag [10], has been shown to result in higher photocatalytic activity.

The application of organic components for the improvement of properties of TiO_2 layers has started relatively recently. Siloxanes are often used due to their elasticity, thermal stability and for some applications to their hydrophobicity [11]. Important properties of these polymers are the low glass point temperature, sufficient environmental resistance, low surface tension and high permeability [12]. Another reason for the implementation of an organic component into inorganic materials is the possibility to prepare thicker layers without multiple coating onto the substrate and simultaneously to maintain the material's desirable properties [6,7]. One of the crucial parameters of the preparation is the annealing temperature. TiO_2/siloxane layers annealed at the temperature lower than 200 °C are practically nonporous, while at 300–400 °C the organic component is decomposed and porosity is formed [7,13,14].

The photocatalytic activity and hydrophilicity of the thin sol–gel layers of TiO_2 can be improved by the addition of SiO_2, which influences both the crystallinity and the surface acidity [15,16]. With the increasing concentration of SiO_2, the particle size of TiO_2 becomes smaller, which is due to barring the

* Corresponding author. Tel.: +420 2 2044 4112; fax: +420 2 2044 4410.
E-mail address: Josef.Krysa@vscht.cz (J. Krýsa).
URL: http://www.vscht.cz

0926-3373/$ – see front matter
doi:10.1016/j.apcatb.2007.10.012

contact among TiO_2 particles by SiO_2 or Ti–O–Si bonds during the growth progress [5,16]. Clearly discernible crystals of anatase are formed up to the concentration of SiO_2 of about 30–40%.

In the manuscript, both mechanical/chemical and photo-induced properties of TiO_2 films modified with two differing additives, namely SiO_2 and polydimethylsiloxane, were compared. In order to assess the application potential of the modified films and to find their strong and soft points, such principally different properties were addressed as crystallinity and mechanical and thermal stability. The photocatalytic activity was tested in two fundamentally different systems, namely in the decomposition of a diluted dye and a solid layer deposited on the film surface. Such a comparison has been done in the literature very rarely, mostly only one system is addressed. We have shown that the different character of additives used has a profound effect on the photocatalytic activity of the films. The advantageous properties of modified films enable their application in respective areas as has been suggested in the manuscript.

2. Experimental

2.1. Chemicals

Titanium isopropoxide (TiP, Sigma–Aldrich) and tetraethoxysilane (TEOS, 98%, Fluka) were used as the sources of the inorganic components of the films, while polydimethylsiloxane (PDMS, $M_n = 550$, Sigma–Aldrich) was the organic part. Tetrahydrofuran (THF, p.a.), isopropanol (IPA, p.a) and acetylacetone (AcAc, p.a.) served as solvents; hydrochloric acid (HCl, 36%) was used as a catalyst. Methylene blue (MB; p.a) was purchased from George T. Gurr, London, UK.

2.2. Preparation of the films and xerogels

The thin films modified either with PDMS or SiO_2 were prepared according to the following procedure. First, one third of the total amount of solvents was mixed with TiP and PDMS or TEOS. Afterwards the solution was homogenized for about 2 h, followed by the addition of the rest of the solvents, demineralised water and hydrochloric acid. The final reaction mixture was aged for 24 h at room temperature under stirring. While the molar ratio H_2O/HCl was fixed at 0.9/0.15 for all the sols, those of TiO_2/PDMS and TiO_2/SiO_2 were varied from 0.7/0.3 to 0.9/0.1. The molar ratio of used solvents and water was H_2O/THF/IPA/AcAc = 0.9/5/5/3. As the substrates, soda lime glass microscope slides with ground edges (Marienfeld, 25.4 mm × 76.0 mm in size and 1–1.2 mm in thickness) were used. Substrates were dip-coated with prepared sols at the room temperature, the immersion rate, the holding time in the sol and the withdrawal rate being 20 cm min^{-1}, 30 s and 6 cm min^{-1}, respectively. Finally, the coated substrates were dried for 30 min at room temperature and calcined at 250–500 °C for 2 h. An overview of prepared layers and their designation is provided in Table 1. The films modified with PMDS and SiO_2 are specified as N and S, the number before and behind the slash corresponding to the molar percentage of the dopant and the temperature of calcination, respectively.

Table 1
The list of prepared films

Sample	Composition	Molar ratio	Temperature of calcination (°C)
N10/250	TiO_2/PDMS	0.9/0.1	250
N10/350	TiO_2/PDMS	0.9/0.1	350
N10/450	TiO_2/PDMS	0.9/0.1	450
N20/250	TiO_2/PDMS	0.8/0.2	250
N20/350	TiO_2/PDMS	0.8/0.2	350
N20/450	TiO_2/PDMS	0.8/0.2	450
N30/250	TiO_2/PDMS	0.7/0.3	250
N30/350	TiO_2/PDMS	0.7/0.3	350
N30/450	TiO_2/PDMS	0.7/0.3	450
S10/350	TiO_2/SiO_2	0.9/0.1	350
S10/450	TiO_2/SiO_2	0.9/0.1	450
S20/350	TiO_2/SiO_2	0.8/0.2	350
S20/450	TiO_2/SiO_2	0.8/0.2	450
S30/350	TiO_2/SiO_2	0.7/0.3	350
S30/450	TiO_2/SiO_2	0.7/0.3	450
S40/350	TiO_2/SiO_2	0.6/0.4	350
S40/450	TiO_2/SiO_2	0.6/0.4	450
S50/350	TiO_2/SiO_2	0.5/0.5	350
S50/450	TiO_2/SiO_2	0.5/0.5	450

For some of the characterization methods powder xerogels were used. These materials were prepared from the identical precursors as the films using identical drying and calcination procedures, which ensures the validity of the data obtained by FT-IR spectroscopy, thermal analysis, X-ray diffraction and nitrogen adsorption also for the respective films. The xerogel are designated analogously to the films.

2.3. Characterization

Infrared spectra of N xerogels were obtained by a FT-IR spectrometer Nicolet 710. The thermal decomposition of xerogels was examined by a Stanton-Redcroft 750 thermo-analyzer (heating rate of 10 °C/min, air atmosphere). The presence of crystalline phases in xerogels was determined by X-ray diffraction using a Seifert XRD 3000 P diffractometer with Co Kα radiation. Adsorption isotherms of nitrogen at 77 K on N xerogels were measured using an ASAP 2010 apparatus (Micromeritic). Prior to the adsorption experiment, samples were outgassed at 250 °C overnight.

The surface morphology and layer thickness were determined by scanning electron microscopy (SEM, Hitachi S4700). The optical properties of the films were measured by UV–vis spectrophotometers Cecil CE 2021 and Perkin-Elmer Lambda 19. The contact angle for water was determined using a CAM-Plus Micro apparatus (Tantec Inc., Schaumburg, USA) and the half-angle measuring method. The adhesion of the coating to the substrate was assessed by the Scotch tape test. An adhesive tape was attached to the coating and the adherence of the coating to the substrate is considered adequate if it is not damaged due to the removal of the tape. The pencil scratch test according to the method H8602 of the Japanese Industrial Standard was used for the assessment of the abrasion resistance.

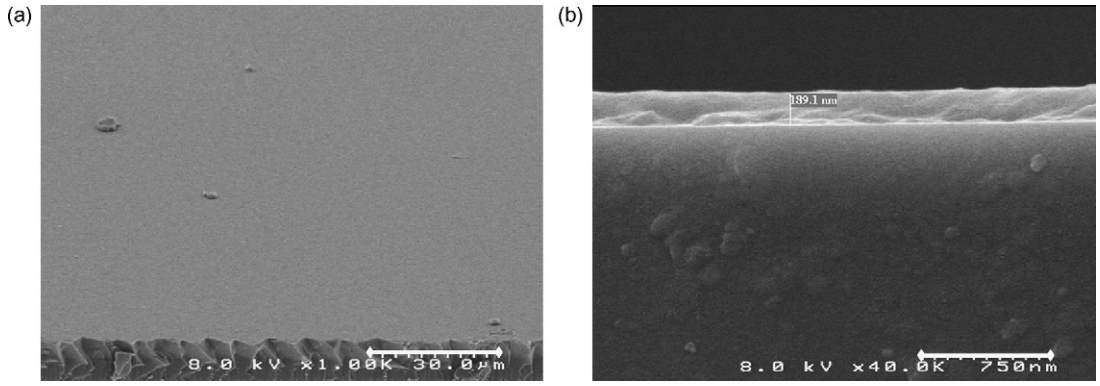

Fig. 1. SEM images of the N20/350 film: (a) top-view; (b) cross-sectional view.

2.4. Photoactivity measurement

For the irradiation experiments, a Sylvania Lynx S 11W BL350 lamp with emission between 320 and 390 nm (broad maximum at 355 nm) was used, the mean incident light intensity being measured by a LT Lutron UV-340 apparatus. The intensity of the irradiation for the photocatalytic and contact angle experiments was 3.2 and 0.5 mW cm^{-2}, respectively.

To test the photocatalytic activity of films prepared, the photodegradation of two model compounds was followed. As a model water pollutant, methylene blue was chosen, while methyl stearate served as a characteristic fatty deposit contaminating solid surfaces.

In the methylene blue test, the dye (2×10^{-5} mol dm^{-3}) was first adsorbed on the film in the dark. Afterwards the adsorption solution was replaced with the test solution (1×10^{-5} mol dm^{-3}) and the films were irradiated with UV light. The concentration of MB in the solution was determined by the UV–vis spectroscopy (the extinction coefficient of methylene blue equals 8.4×10^5 dm^3 mol^{-1} cm^{-1} [17]). In the methyl stearate test, 10 μl of its 20 mM solution in *n*-hexane was first deposited on the film using micropipette. After the evaporation of the solvent at room temperature, the films were irradiated with UV light for 2, 4, 8 and 22 h. Then each sample was extracted with 900 μl of *n*-hexane for 30 min. The concentration of methyl stearate was measured by gas chromatography using a HP-Pona chromatographic column (100% dimethylpolysiloxane, 50 m × 0.2 mm × 0.5 μm) at 250 °C. Injector and detector were heated up to 280 and 250 °C, respectively.

3. Results and discussion

3.1. Characterization of produced materials

All the prepared films were compact, uniform and transparent, their thickness being about 100 nm (S films) and about 200 nm (N films), respectively. The reason of the difference in the thickness is in the different viscosity of used sols. All the layers exhibit an excellent adhesion to the glass support. SEM images for the N and S films are very similar to each other, the surface being very smooth with only few irregularities. As an example, SEM image of the film N20/350 is shown in Fig. 1.

The abrasion resistance of N films depends on the calcination temperature. The lowest resistance was obtained for the film calcined at 250 °C being scratched with the softest pencil (8B – mark 1 from 20 in the scale of pencil hardness), while films calcined at 350 and 450 °C resist the pencil as hard as 5H (mark 15). The S films exhibit significantly higher abrasion resistance, which does not depend on the calcination temperature in the

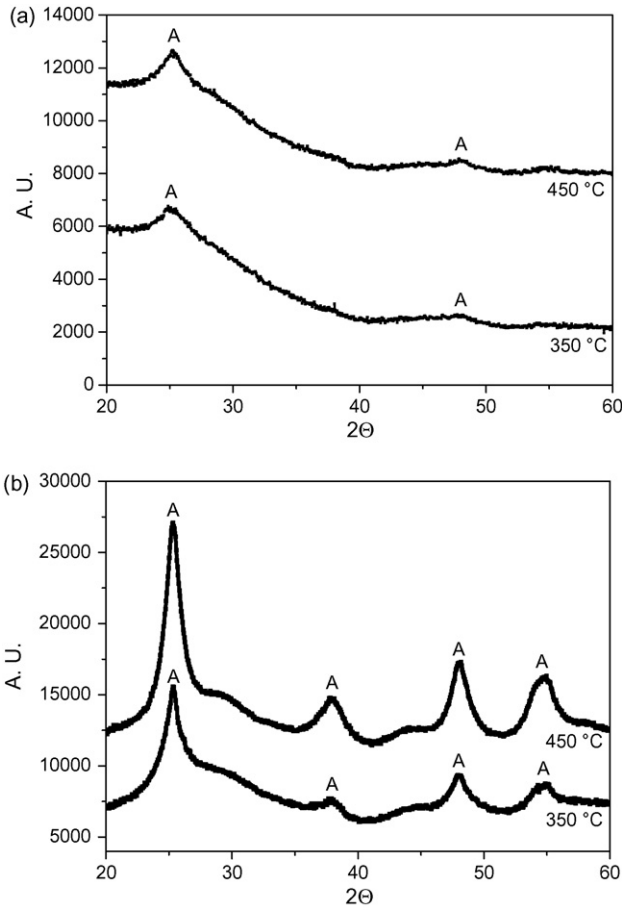

Fig. 2. X-ray diffractogram of N20 (a) and S20 (b) xerogels calcined at different temperatures.

range from 250 to 450 °C. All the films withstand the scratching with the hardest pencil (10H – mark 20 from 20 in the scale of pencil hardness), the percentage of SiO_2 having no effect.

The crystallinity of the films depends on their chemical composition and the temperature of the heat treatment. X-ray diffractograms of N20 and S20 xerogels calcined at different temperatures are shown in Fig. 2a and b, respectively. The sample N20/350 is practically amorphous, the content of anatase being less than 5%. Due to the detection limit and significant content of amorphous phase in the N20 samples the crystal size cannot be determined by the Scherrer equation with sufficient precision. With rising calcination temperature, the percentage of anatase increases only slightly. It means that even if PDMS is decomposed at temperatures 350–450 °C, only very limited crystal growth was detected (Fig. 2a). The reason is the inhibition effect of the highly dispersed SiO_2, which is formed due to the PDMS decomposition.

In contrast to the N20 samples, the content of anatase in the samples S20 calcined at 350 and 450 °C is much higher. The percentage of anatase increases significantly with rising calcination temperature but the crystal size only slightly from 3 to 5 nm.

The results of TG/DTA analysis for powder xerogels N20 and S20 are shown in Fig. 3a and b, respectively. For the N20 xerogel the decrease in weight up to 100 °C can be attributed to the desorption of physisorbed water (confirmed by an endothermic peak on the DTA curve at about 100 °C). This is followed by the removal of organic solvents at 100 to 350 °C. Above 250 °C the weight starts to decrease very rapidly, which

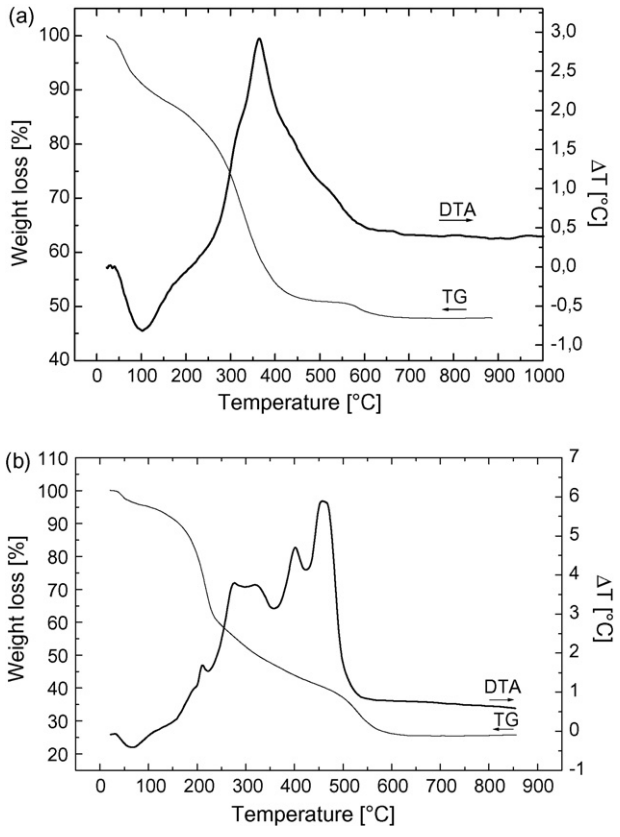

Fig. 3. TG and DTA curves of N20 (a) and S20 (b) xerogels.

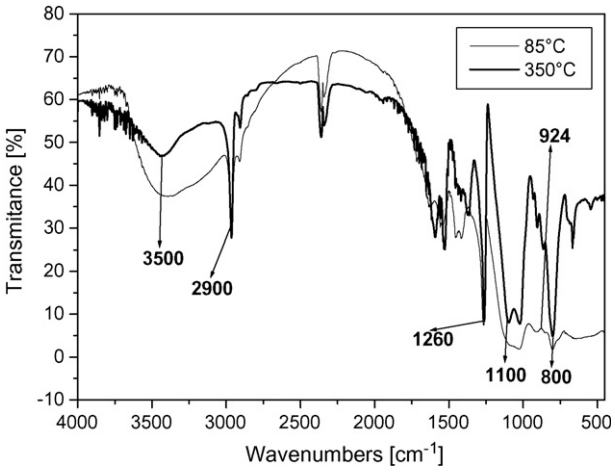

Fig. 4. FTIR spectra of N20/85 and N20/350 xerogels.

is due to the decomposition of polydimethylsiloxane (confirmed by an exothermic peak on the DTA curve at about 370 °C), which is in agreement with the published data [11]. Above 400 °C, the change in weight is very small [6,11].

For the S20 xerogel the results of TG and DTA analysis are different. Under 100 °C the endothermic evaporation of physisorbed water occurs. The fast decrease in weight at 150–200 °C is due to the desorption of the main part of organic solvents, followed with less steep section at 200–500 °C [18,19]. The corresponding part of the DTA curve is very complex, suggesting several exo- and endothermic processes. Exothermic peaks are due to both the removal of the rests of the solvents and the decay of the unhydrolysed ethoxy- and isopropoxy-groups [18]. The endothermic processes are caused by the formation of OH groups from hydrolysed alkoxyde groups. At cca 475 °C the exothermic crystallization of the amorphous TiO_2 to crystalline anatase takes place. Finally the decrease in weight at 500–600 °C is due to the dehydroxylation of the surface and formation of oxygen bridges.

FT-IR spectra of the N20/85 and N20/350 xerogels are shown in Fig. 4. For the sake of sample characterization, some typical peaks from the spectrum were selected. The absorption peak at around 3500 cm^{-1} corresponds to hydroxyl group, as expected its size is decreasing with the increasing temperature of treatment. It means that increasing calcinations temperature results in surface dehydroxylation which further corresponds to the results of contact angle measurement. While the absorption peaks at 2900 and 1260 cm^{-1} correspond to methyl groups, those at around 800 and 1100 cm^{-1} are assigned to symmetric and asymmetric Si–O–Si stretching vibrations in siloxane network [7,11]. Their presence at both temperatures confirms that inorganic–organic character remains till 350 °C. In addition, there is an absorption peak at 924 cm^{-1} corresponding to the Si–O stretching vibrations of Si–OH and/or the vibrations of Si–O–Ti bonds [6]. An existence of Si–O–Ti bond verifies the formation of three-dimensional structure with interconnected inorganic and organic component.

The comparison the adsorption isotherms on xerogels N20/350 and N20/450 clearly shows that the character of their

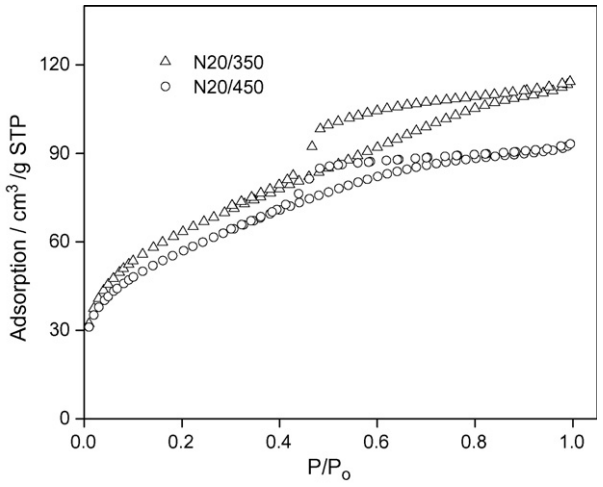

Fig. 5. Adsorption isotherms of nitrogen at 77 K on N20/350 and N20/450 xerogels.

texture is practically identical. There is only small difference in the BET surface area and total pore volume: 222 and 200 m^2/g, and 0.177 and 0.144 cm^3/g for N20/350 and N20/450, respectively. The comparative plots for both samples (Fig. 5) unequivocally prove that both of them contain very similar proportion of micropores, namely 0.028 and 0.030 cm^3/g for N20/350 and N20/450, respectively. As the reference adsorbent several materials have been tested, both titania and silica gels. In the end, macroporous silica gel Davisil (Supelco) was selected. The criterion for this choice is the practically linear course of the plot in Fig. 6, which testifies the identity of the adsorption process on both tested and reference materials. Titania seems less suitable as a reference material because it is a crystalline material as opposed to the low crystallinity of N20 materials. The shape of the hysteresis loop for both samples clearly indicates some pore blocking, as the almost horizontal plateau of adsorption ends with an abrupt downwards turn at P/P_0 of ca 0.43 (the tensile strength limit). Therefore, it can be

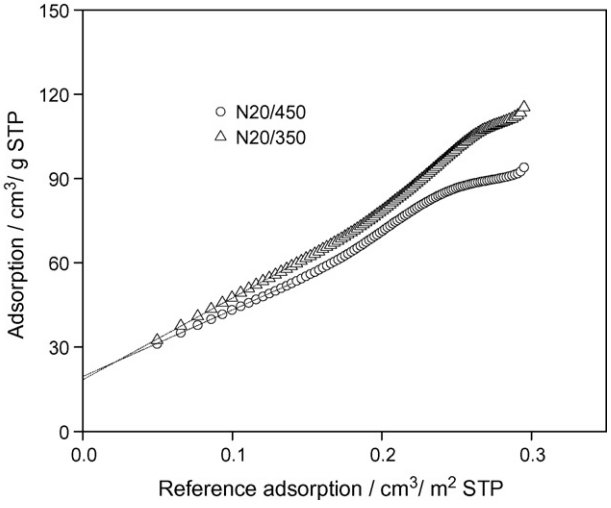

Fig. 6. Comparative plots for N20/350 and N20/450 xerogels. Reference isotherm on silica gel Davisil 663XWP (Supelco), BET surface area = 82.8 m^2/g.

Table 2
The contact angles for water of the N- and S-series of samples measured in dark

Sample	Temperature of calcination (°C)	Contact angle for water (°)
N10	250	74
N10	350	54
N10	450	54
N20	250	78
N20	350	49
N20	450	36
N30	250	85
N30	350	47
N30	450	40
TiO_2	350	23
S10	350	15
S10	450	67
S20	350	11
S20	450	67
S30	350	8
S30	450	54
S40	350	7
S40	450	51
S50	350	4
S50	450	65

concluded that the porosity of both samples is characterized by some cavities which are connected with each other and with the external surface via narrow pores, the so-called ink-bottle type of porosity. The cavities are being created by the partial decomposition of the organosiliceous component of the material. The slightly lower surface area and pore volume of the samples calcined at the higher temperature of 450 °C is due to some additional thermal sintering or destruction.

3.2. Wetting properties of the films

3.2.1. In dark

Table 2 gives the contact angle for water for all the samples studied. The measurement over the whole area of the films (10 points) has shown that the films are uniform, the standard deviation of the contact angle being 3–5°. The contact angle for pure glass was 33°. The deposition of a N film results in an increase of the contact angle but its value is not much influenced by the percentage of PDMS. However, an increase in the calcination temperature has led to a substantial decrease in the contact angle. While the films calcined at 250 °C are almost hydrophobic, those calcined at 450 °C are slightly hydrophilic with the contact angle mostly under 50°. This change in contact angle is clearly due to the decomposition of the hydrophobic PDMS component and the formation of highly dispersed SiO_2.

The S films calcined at 350 °C are much more hydrophilic, their contact angle for water decreasing with the increasing concentration of SiO_2, from 15 to 4° for the layers containing 10 and 50 mol.% of SiO_2. The addition of SiO_2 to TiO_2 results in increased surface acidity and consequent enhancement of the surface hydrophilicity as proposed by Guan [16]. However, the S films calcined at 450 °C are relatively hydrophobic, their contact angle ranging from 50 to 70° without any clear dependence on the content of SiO_2. The increase in

Table 3
The photoinduced superhydrophilicity of S-series films calcined at 450°C

Sample	Contact angle for water (°)	Contact angle for water after UV irradiation (°)	Contact angle for water after a week's storage in dark (°)
S10	67	~5	66
S20	67	~5	57
S30	54	~5	43
S40	51	~5	23
S50	65	~5	28

hydrophobicity is obviously due to the dehydroxylation of the film surface.

3.2.2. *Effect of the UV irradiation*

The UV illumination has practically no effect on the wetting properties of the N films, i.e. the PDMS-modified films do not exhibit the illumination induced increase in hydrophilicity well known for the TiO_2 materials. On the other hand, all the S films exhibit very marked photoinduced superhydrophilicity, the light intensity of 0.5 mW cm^{-2} being sufficient to decrease the contact angle for water below 5° (Table 3). After a week's storage in dark, the contact angle for water has increased, the increase depends on the content of SiO_2. While the contact angle for film containing 10% has returned to its value before illumination, those for films with 20–30% of SiO_2 are much lower. The films with the highest content of SiO_2 (40–50%) are very hydrophilic, the water even drop trickling at the inclined film. The stability of the photoinduced hydrophilicity clearly depends on the content of SiO_2, roughly the higher the content the more stable the hydrophilicity (Table 3). The optimum long-term photoinduced hydrophilicity was achieved for the SiO_2 content of 30%, which is close to the published data by Guan [16], who found the 30–40% SiO_2 addition as an optimum.

The addition of silica at higher concentration levels has several effects. It prevents the recrystallization of the titania component and the formation of large crystals of anatase. SiO_2 also increases the Lewis acidity of the composite oxide resulting in the increasing hydroxyl coverage of the surface. According to a model proposed by Inagaki et al. [20], it is due to the charge imbalance caused by the replacement of Ti with the coordination number of 6 with Si, whose coordination number is only 4. The stable silanols ensure sufficient water trapping and consequently also the hydrophilicity of the surface even if the titanols have partially lost their efficiency due to the desorption or the blocking by adsorbed impurities.

3.3. *Photocatalytic activity*

Methylene blue ($C_{16}H_{18}ClN_3S.3H_2O$), used in textile industry and in microscopy, often serves as a model compound for the photoactivity measurement [20–22]. Notwithstanding, there are only few papers describing in detail the mechanism of its photocatalytic degradation. The dye is first adsorbed on the photocatalyst surface and then oxidized by photoinduced holes to a radical $MB^{\bullet+}$ [23]. The latter reacts further with O_2 to a radical $[MBOO^{\bullet}]^{+}$ and then to thionine. Finally, the hetero-polyaromatic ring is broken, and aniline and 4-nitroaniline are formed [17].

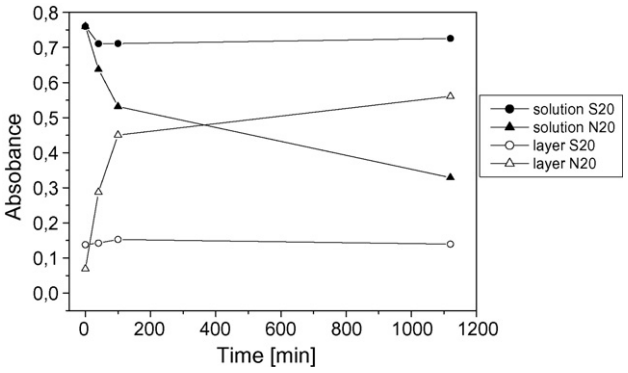

Fig. 7. The kinetics of the methylene blue adsorption on S20/350 and N20/350 thin films expressed as the time evolution of the absorbance at 664 nm for the MB solution in dark.

Photocatalytic activity was measured on S20/350 and N20/350 films. First dye was adsorbed on the film surface from its water solution. Fig. 7 shows the kinetics of the dye adsorption as the change in the MB absorbance at 664 nm both in the solution and the thin film. For both films, the concentration of MB in the solution decreases, while that in the film increases. For the S20/350 film an equilibrium was achieved after about 100 min, while for the N20/350 much longer time was needed. The amount of adsorbed MB on the N20/350 film is much larger than that on the S20/350 one, which suggests an important role of the nature of the additive and is in agreement with the developed porosity and large surface area of the N films.

Fig. 8 shows the dependence of the methylene blue concentration in the solution for N20/350 and S20/350 films on the UV irradiation time. The S20/350 film exhibits substantially higher degradation rate. It seems to be due to its higher crystallinity (Fig. 2) and its high hydrophilicity (Table 2), which is further enhanced by the UV-illumination

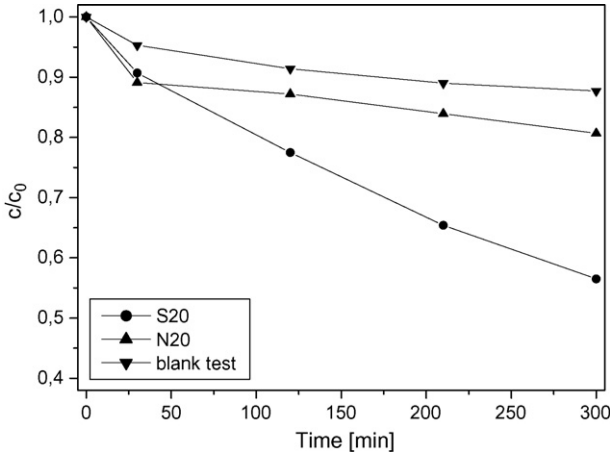

Fig. 8. The kinetics of the photocatalytic degradation of methylene blue on N20/350 and S20/350 films expressed as the time evolution of the MB concentration in the solution.

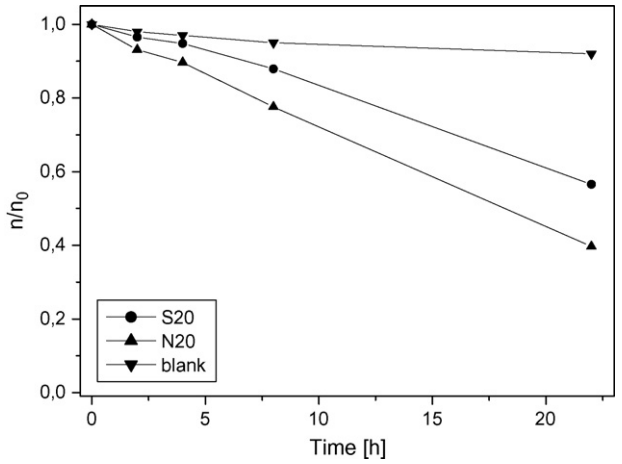

Fig. 9. The time evolution of the molar concentration of methyl stearate deposited on the S20/350 and N20/350 films during UV-illumination.

and the conversion into the superhydrophilic state. The photocatalytic activity of the N20 films is much lower being almost comparable with the blank sample. The possible explanation is the low crystallinity of the film and especially its adsorption properties towards MB due to its developed porosity. The very high surface concentration of the compound to be degraded seems detrimental as the intermediates of the parent compound's decomposition also adsorbed on the surface may limit the rate of the photocatalytic reaction. It is exactly the case for MB whose first degradation product is thionine. It has been found that the formation of TH as a very stable intermediate in the photocatalytic degradation of MB appears to be a special feature of films with a large surface area, such as N20 [24]. Apparently, the optimum photocatalytic efficiency is achieved when the dye is adsorbed to some extent thus enabling its decomposition directly through the transfer of holes, while, on the other hand, the photocatalytic degradation process is also initiated in the homogenous solution phase, e.g., as by secondary species such as $O_2^{\bullet -}$ and $HO_2^{\bullet}$ [24].

Fig. 9 shows the photocatalytic activity of the same two films (S20/350 and N20/350) in the decomposition of methyl stearate. For the sake of comparison, a blank experiment (irradiated film of methyl stearate on glass support) is also shown. In this reaction the photocatalytic efficiencies are reversed. The N20/350 film exhibits substantially higher degradation rate than S20/350. Also in this case the reason seems to be the film porosity. In the decomposition of solid compact layers deposited on the surface of the photocatalyst the rate-determining step is very often the diffusion of oxygen and water vapor. It seems that the developed mesoporosity substantially enhances this diffusion even if the external surface is blocked by the deposited layer.

4. Conclusions

It has been shown that the nature of the additive has decisive effect on the properties of TiO_2/PDMS and TiO_2/SiO_2 films. TiO_2 films modified with PDMS exhibit lower abrasion resistance and are relatively hydrophobic (contact angle for water of about 50°). They exhibit developed micro-mesoporosity, which substantially enhances the adsorption of methylene blue but is detrimental in the dye decomposition. On the other hand, these films are highly efficient in the decomposition of methyl stearate which is also due to the developed porosity enhancing the diffusion of viable species.

The abrasion resistance of films modified with SiO_2 is much better. Due to their hydrophilic properties they are good catalysts for the degradation of methylene blue. Moreover, they can be easily converted by weak UV-illumination into superhydrophilic state, which is substantially stable. Due to the mentioned properties and their excellent transparency these films are promising candidates for the application as self-cleaning layers on glass and ceramic materials.

Acknowledgments

The authors thank the Ministry of Education, Youth and Sport of the Czech Republic (project 1M0577) for the financial supports.

References

[1] C.J. Brinker, G.W. Scherer, Sol–Gel Science, The Physics and Chemistry of Sol–Gel Processing, Academic Press, San Diego, 1990.
[2] M.R. Hoffmann, S.T. Martin, W. Choi, D. Bahnemann, Chem. Rev. 95 (1995) 69.
[3] A. Fujishima, K. Hashimoto, T. Watanabe, TiO_2 Photocatalyst, Fundamentals and Applications, BKC, Tokyo, 1999.
[4] J. Yu, J.C. Yu, X. Zhao, J. Sol–Gel Sci. Technol. 24 (2002) 95.
[5] K. Guan, B. Lu, Y. Yin, Surf. Coat. Technol. 173 (2003) 219.
[6] W. Que, Z. Sun, Y. Zhou, Y.L. Lam, Y.C. Chan, C.H. Kam, Thin Solid Films 359 (2000) 177.
[7] W. Que, X. Hu, Q.Y. Zhang, Chem. Phys. Lett. 369 (2003) 354.
[8] J. Liqianga, F. Hongganga, W. Baiqia, W. Dejunb, X. Baifua, L. Shudana, S. Jiazhong, Appl. Catal. B Environ. 62 (2006) 282.
[9] I.-H. Tseng, J.C.S. Wu, H.-Y. Chou, J. Catal. 221 (2004) 432.
[10] I.M. Arabatzis, T. Stergiopoulos, M.C. Bernard, D. Labou, S.G. Neophytides, P. Falaras, Appl. Catal. B: Environ. 42 (2003) 127.
[11] T. Shindou, S. Katayama, N. Katayama, K. Kamiya, J. Sol–Gel Sci. Technol. 27 (2003) 15.
[12] J.M. Breiner, J.E. Mark, Polymer 39 (1998) 5483.
[13] S. Dire, F. Babonneau, G. Carturan, J. Livage, Non-Cryst. Solids 147–148 (1992) 62.
[14] S. Dire, R. Ceccato, F. Babonneau, J. Sol–Gel Sci. Technol. 34 (2005) 53.
[15] J. Yu, J.C. Yu, X. Zhao, J. Sol–Gel Sci. Technol. 24 (2002) 95–103.
[16] K. Guan, Surf. Coat. Technol. 191 (2005) 155–160.
[17] M. Itoh, H. Hattori, K. Tanabe, J. Catal. 35 (1974) 225.
[18] L. Zhao, J. Yu, B. Cheng, J. Solid State Chem. 178 (2005) 1820.
[19] J. Yu, L. Zhao, B. Cheng, Mater. Chem. Phys. 96 (2006) 313.
[20] M. Inagaki, T. Imai, T. Yoshikawa, B. Tryba, Appl. Catal. B: Environ. 51 (2004) 247.
[21] R.S. Sonawane, S.G. Hegde, M.K. Dongare, Mater. Chem. Phys. 77 (2003) 744.
[22] K. Iketani, R.-D. Sun, M. Toki, K. Hirota, O. Yamaguchi, Mater. Sci. Eng. B 108 (2004) 187.
[23] T. Zhang, T. Oyama, A. Aoshima, H. Hidaka, J. Zhao, N. Serpone, J. Photochem. Photobiol. A: Chem. 140 (2001) 163.
[24] J. Tschirch, D. Bahnemann, M. Wark, J. Rathouský, J. Photochem. Photobiol. A: Chem. (2007) in press.